doi:10.1017/S1431927611004570
Microsc. Microanal. 17 (Suppl 2), 2011

Non-Tangential Continuity Reconstruction in Atom Probe Tomography Data

D.J. Larson, B.P. Geiser, T.J. Prosa, R.M. Ulfig and T.F. Kelly

Cameca Instruments Inc., 5500 Nobel Drive, Madison, WI 53711

A shank angle reconstruction [3] is useful in atom probe tomography (APT) in cases where there is no direct correlation between specimen curvature and the voltage required for field evaporation, particularly in the case of complex specimens [4]. In APT data reconstruction, the standard assumptions often include a hemispherical evaporating surface and a tangential continuity restriction between this surface and the specimen shank region [1-3]. By improving the geometry we can make reconstructions more accurate when using physical measurements of the specimen as input.

Under the tangential continuity assumption, there is a simple relationship between R_{tip} and R_{cone} (Fig. 1): $f_{s/c} \equiv R_{tip}/R_{cone} = \sec \alpha$. Blavette *et al*. [1] has described the formula for evolving the tip radius with analysis depth as $dR_{tip}/dz_{tip} = \sin \alpha / (1 - \sin \alpha) \equiv K_\alpha$. As observed experimentally [4-7], field-evaporated specimens do not necessarily assume a shape with tangential continuity. Fig. 2 shows a specimen with $f_{s/c}$=1.5, although values with vary from specimen to specimen [6]. If this constraint is removed (as shown in Fig. 3), we can generalize the dR_{tip}/dz term as:

$$K_{\alpha,f} \equiv \frac{\tan(\alpha) f_{s/c}}{1 - \tan(\alpha) f_{s/c} + \tan(\alpha)\sqrt{f_{s/c}^2 - 1}}.$$

Fig. 4 shows the behavior of the dR_{tip}/dz term as a function of shank angle over a range of $f_{s/c}$ values. Fig. 5 shows this dependence as normalized to the case of $f_{s/c} = \sec \alpha$. It is important to note that the formulas for reconstruction do not change with this constraint on the specimen geometry since all effects of the radius evolution are absorbed into K_α (previously denoted as "*w*" in [3]). Fig. 6 shows the dependence of the variation in interplanar spacing with analysis depth as derived from [3]. Fig. 7 provides an experimental comparison (as measured by spatial distribution mapping [8]) with analysis depth from a simulation of aluminum (<100> spacing of 0.204 nm). For these results we have used R_0 = 20 nm and a range of shank angles, assuming the evaporation shape has $f_{s/c}$ = 1.5.

As noted above, the effect of non-tangential continuity (and shank angle) is contained entirely within K_α, and is more significant for small tip radii. It is instructive to consider the change in shank angle that is required (for a variety of $f_{s/c}$ values) if a reconstruction constrained to tangential continuity is imposed. Fig. 8 shows that when tangential continuity is assumed, the angles that must be used for accurate reconstruction are larger than values obtained from high-resolution microscopy.

In summary, assumptions of tangential continuity bias reconstructions toward parameters with unphysically large shank angles. The new developments contained in the current work enable APT reconstructions to take advantage of electron microscopy-based information about the real physical size of specimens as well as shank angle and the level of discontinuity between the apex and the shank ($f_{s/c} \neq \sec \alpha$) to provide constraints on the selection of reconstruction parameters.

[1] D. Blavette et al., *Revue Phys. Appl.* 17 (1982) 435.
[2] P. Bas et al., *Appl. Surf. Sci.* 87/88 (1995) 298.
[3] B. P. Geiser et al., *Micro. Microanal.* 15(S) (2009) 292.
[4] E. A. Marquis et al., *J. Microscopy* (2011) doi: 10.1111/j.1365-2818.2010.03421.x.
[5] S.S.A. Gerstl et al., *Micro. Microanal.* 15(S2) (2009) 248.
[6] A. Shariq et al., *Ultramicroscopy* 109 (2009) 472.
[7] D. J. Larson et al., *J. Microscopy* (2011) doi: 10.1111/j.1365-2818.2010.03474.x.
[8] B. P. Geiser et al. *Micro. Microanal.* 13(6) (2007) 437.

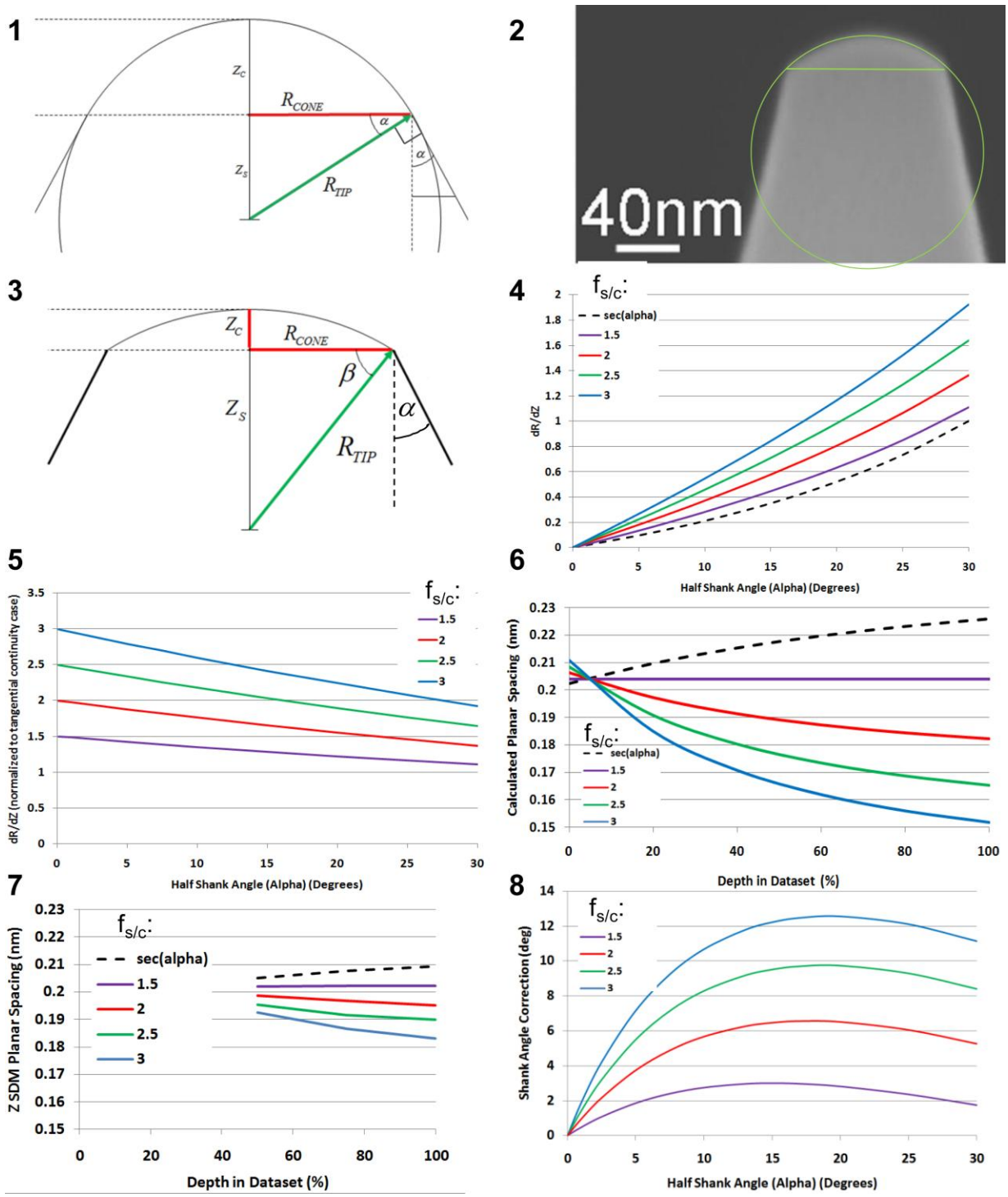

Fig. 1. Schematic description of tangential continuity between hemisphere and cone.
Fig. 2. Scanning electron microscopy image of field evaporated surface (from [6]).
Fig. 3. Schematic description of non-tangential continuity between hemisphere and cone.
Fig. 4. $K_{\alpha f}$ (dR_{tip}/dZ)term as a function of shank angle.
Fig. 5. Data from Fig. 4 normalized to the tangential continuity condition of $f_{s/c}$ = sec α.
Fig. 6. Dependence of the variation in interplanar spacing with analysis depth (dashed line shows $f_{s/c}$ = sec α).
Fig. 7. Experimental comparison to Fig. 6 (as measured by spatial distribution mapping) from simulated aluminum.
Fig. 8. Shank angle correction required if data reconstruction constrained to tangential continuity is imposed.

https://doi.org/10.1017/S1431927611004570 Published online by Cambridge University Press